THE ASTROPHYSICAL JOURNAL, 195:269–277, 1975 January 15

THE SPECTRUM OF OH 471 (0642+44)

R. F. CARSWELL, P. A. STRITTMATTER,* AND R. E. WILLIAMS
Steward Observatory, University of Arizona
AND
E. A. BEAVER AND R. HARMS
Department of Physics, University of California, San Diego
Received 1974 July 17

ABSTRACT

Results of image-tube and Digicon spectroscopy of OH 471 (0642+44) are reported. Wavelengths of 89 stronger absorption features in the range 4000–6000 Å are given, and a number of absorption redshift systems are suggested. The lack of radiation shortward of 4000 Å is attributed to Lyman continuum absorption in the gas giving rise to the various absorption-line systems.

Subject headings: line identifications — quasi-stellar sources of objects — redshifts

I. INTRODUCTION

The radio source OH 471 (0642+44) was identified by Gearheart *et al.* (1972) and by Browne, Crowther, and Adgie (1973) with an 18.5–19 mag neutral stellar object which was subsequently found to have an emission-line redshift $z_{em} = 3.40$ (Carswell and Strittmatter 1973). The spectrum, which contains numerous absorption lines, is of special interest because the continuum radiation declines steeply at wavelengths shortward of the redshifted Lyman limit, a feature so far unique among known QSOs.

II. THE OBSERVATIONAL MATERIAL

We have obtained three well-widened spectra (SI 857, 859, 869) of OH 471 at a reciprocal dispersion $d = 90$ Å mm^{-1} using the Cassegrain spectrograph and RCA 33063 image tube at the Steward Observatory 2.2-m telescope. This system gives an effective resolution $r \sim 4$ Å and covers the spectral range 3600–5500 Å. These data have been supplemented by measures of two earlier lower-dispersion spectra (SI 835, SI 856, $d \sim 240$ Å mm^{-1}, $r \sim 10$ Å) which yielded a few strong features longward of 5500 Å.

In addition, two Digicon scans of OH 471 were obtained in 1974 February using the UCSD 40-element device attached to the same spectrograph. The detector has been described by Beaver and McIlwain (1971). The scans cover the spectral regions 3630–4670 Å and 4420–5470 Å, respectively, with an effective resolution $r \sim 24$ Å. The image was quarter-stepped along the diode array to ensure adequate sampling. The observation periods (2^h and 1^h30^m for the blue and red scans, respectively) were divided into many shorter intervals of approximately equal total duration on OH 471 and the sky. The uncorrected data for OH 471 plus sky and sky alone are shown in figure 1. The results for the object spectrum after calibration and numerical filtering are shown in figure 2, where the dashed lines correspond to $\pm\sigma$ deviations of the mean (filtered) curve.

The (small) diode-to-diode differences were calibrated out by comparison with a standard lamp. In no case did these corrections amount to more than 10 percent. The net object counts n_i and the associated statistical error σ_i at position i were taken to be

$$n_i = n_{0,i} - n_{s,i}$$

and

$$\sigma_i = (n_{0,i} + n_{s,i})^{1/2} ,$$

where $n_{0,i}$ and $n_{s,i}$ denote the number of counts, after diode-to-diode corrections, in the object and sky channels, respectively.

The data were then filtered numerically with a trapezoidal filter function and interpolated (for convenience in plotting) at points corresponding to one-eighth of a diode interval. With the origin of x centered on such an interpolation point and with x in units of the measuring interval (one quarter diode spacing), the weighting factors for the filter are given by

$$w = a \qquad (x \leq 1.5) ,$$
$$w = a(2.5 - x) \qquad (1.5 \leq x \leq 2.5) ,$$
$$w = 0 \qquad (x \geq 2.5) ,$$

where a is a normalizing constant such that $\sum w = 1$. This filter has a width corresponding approximately to a diode width and has the effect of increasing the effective signal-to-noise by suppressing Fourier components in the measured spectrum with wavelengths smaller than the diode interval. The error σ in the interpolated point was computed as

$$\sigma = \sum w_i^2 \sigma_i^2 ,$$

and this was used to compute the confidence envelope shown in figure 2. A final correction was made to take

* Alfred P. Sloan Research Fellow.

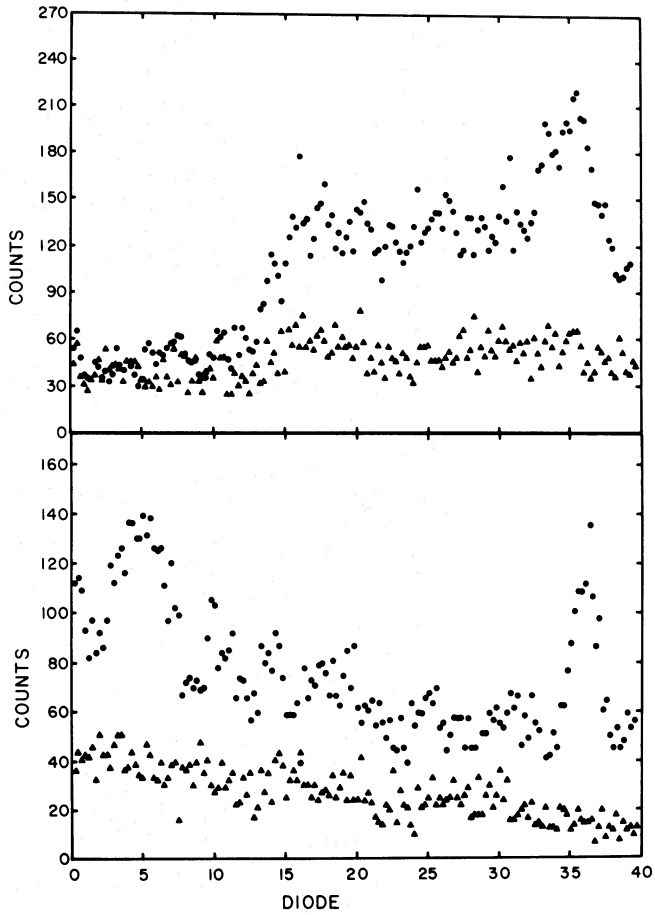

FIG. 1.—The original Digicon data for blue and red scans are shown as a function of diode position

out the overall variation in sensitivity of the entire system as a function of wavelength. Observations were made of one or more nearby white dwarfs for which Oke (1974*a*) has provided absolute spectrophotometry. Ratios of expected to observed counts per angstrom were computed at Oke's calibration wavelengths, and a least-squares fit was made to a polynomial response curve. The filtered data were then corrected using this response curve, and the results are those shown in figure 2.

Wavelengths of measured absorption features on each of the three image-tube spectra are listed in table 1 together with adopted wavelengths and estimates of line strength and width. Each spectrogram was analyzed independently and clear features were noted; these features are entered without brackets under the appropriate spectrogram number in table 1. The data were then collated and a search made to see whether lines present on at least one spectrogram had been "missed" on others. If a "missing" feature was then found, it is entered in brackets in table 1. Spectrogram SI 857 was rather underexposed, so no useful data could be obtained longward of ~4700 Å. Lines are deemed definite only if they appear similar on all spectrograms for which the appropriate spectral region is well exposed. The wavelengths of such lines are entered without brackets in column (4) of table 1. Lines for which some question exists, usually weak lines which do not appear on one spectrogram or lines with greatly differing strength on different plates are entered in parentheses in column (4). No meaningful description of these features can, of course, be given. Both SI 859 and SI 869 are overexposed in the region of O VI emission (4500–4600 Å), which makes weaker features very difficult to detect. This may account for the paucity of "certain" features in this region.

In attempting to compile this line list, we encountered considerable difficulty in deciding when features were single or multiple. This is inevitable in a rich absorption spectrum such as that of OH 471, but it can lead to severe problems when attempting to determine absorption systems. A broad "feature" to which a single mean "wavelength" has been assigned may be made up of many individual lines, in many redshift systems. The assigned wavelength may, in fact, not "agree" very well in any of the redshift systems. Features which contain obvious structure

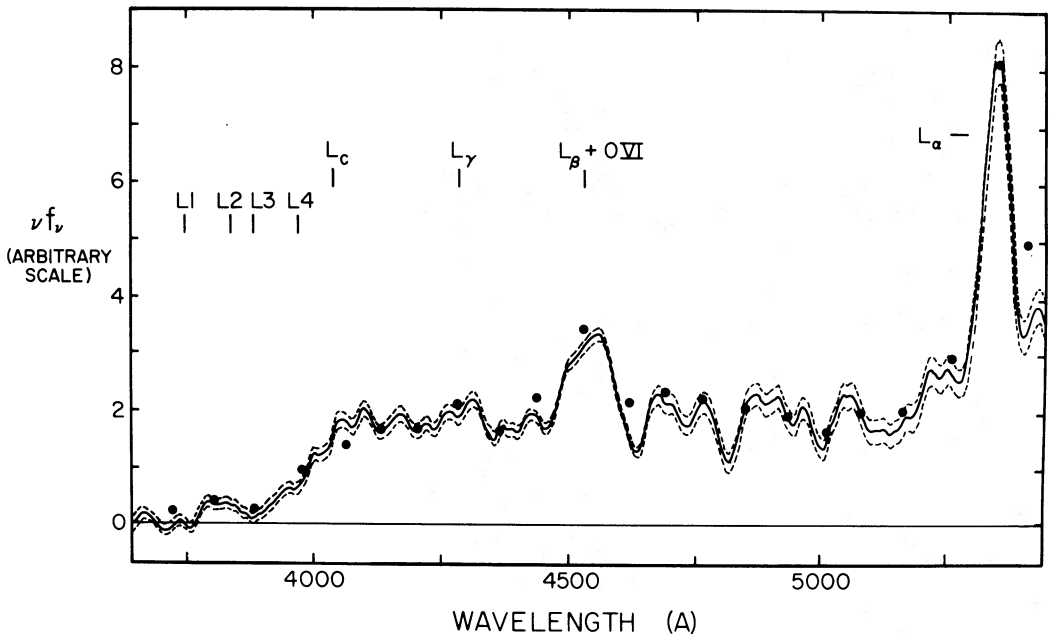

FIG. 2.—The solid central line represents the best interpolated spectrum of OH 471 after calibration and numerical filtering as described in the text. The dashed lines on either side of this denote $\pm 1\sigma$ errors in the smoothed spectrum. The smoothing technique has removed structure over a wavelength interval of less than ~ 30 Å. The positions of the Lyman continuum edge in the emission and the four probable absorption systems are shown as L_c and L1–4, respectively. The vertical scale is in units of photons per A (or νf_ν) on a linear scale; these units are convenient since they (*a*) are those we measure and (*b*) give a measure of the energy in each part of curve. The dots represent observations by Oke (1974*b*).

(i.e., that are incipiently resolved at 90 Å mm^{-1}) are denoted by the letter S in column (6) of table 1. Attempts to obtain higher-resolution spectra of OH 471 are now in progress.

III. THE EMISSION SPECTRUM

Two strong emission line features at ~ 4500 and ~ 5340 Å were noted by Carswell and Strittmatter (1973) and identified with O VI $\lambda 1033.7$ and Lα, respectively. They are clearly visible on the Digicon scans and all spectrograms. Wavelengths of broad emission lines are, however, rather hard to measure accurately, particularly if they are strongly distorted by absorption features. Three low-dispersion spectrograms of OH 471 yield mean central wavelengths λ_c of 4549 and 5352, respectively, for the two strong lines with a total scatter of 3 Å in each case; the lines are, however, overexposed, and structure in the central regions is therefore impossible to measure. The Digicon data avoid the latter difficulty, and determinations of central wavelength λ, equivalent width W, full width at half-maximum $w_{1/2}$, and width at continuum level w_c, are listed in table 2. The main source of error in W, $w_{1/2}$, and w_c is the location of the continuum level. Although there is some discrepancy between the central wavelengths observed photographically and those determined from the Digicon, it is not clear whether this is due to systematic errors in the Digicon wavelength calibration process or to the influence of absorption lines and saturation effects in the photographic data. The ratio of central wavelengths do, however, agree very well, yielding a mean value 1.1766 compared with the Lα/O VI ratio of 1.1761. The corresponding redshifts from the Lα line are 3.397 and 3.402 for the Digicon and photographic data, respectively. The redshift for the second strong feature depends on whether or not there is a significant contribution from Lβ, a question to which we shall return subsequently.

Weaker emission features are also present on the image-tube spectra at ~ 5460 and ~ 6820 Å and may be identified with N V $\lambda 1240$ and C IV $\lambda 1550$, respectively. Since the former is confused with the nightsky Hg I $\lambda 5465$ feature and the latter is at a wavelength at which the response of the RCA tube is declining rapidly, they provide little unambiguous redshift information. The Digicon data contain evidence for the N V feature at 5454 Å giving a redshift $z = 3.396$ which is consistent with that determined for Lα.

It is clearly of interest to inquire whether other members of the Lyman series are present in emission. The results in table 2 indicate that the width of the O VI feature is almost double that of Lα. It is therefore tempting to try to account for the extra breadth of the O VI features in terms of an additional contribution from Lβ. There is, however, no evidence in the measured wavelengths for such a hypothesis—provided both components of the O VI doublet are optically thin. Based on the Lα emission redshift, the predicted wavelength of O VI falls very near the center of the observed feature. The extent of the emission toward longer wavelengths has to be explained in any case, so an appeal to Lβ to account for the blueward

TABLE 1

ABSORPTION LINES IN OH 471

SI 857	SI 859	SI 869	Adopted	Character	Comments
	(3986)	3984	(3984)		
4008	4006	4006	4007	MS/mw	S
4028-35	4032	4032	4032	S/w	S
(4056)	4057	4056	4056		
4073	4073	4073	4073	MS/m	
(4091)	4094	--	(4094)		
4101		4100	(4100)		
4119	4121	4123	4121	M/m	S
(4130)	4129	4130	4130	M/m	S
4145	4144	4145	4145	MS/m	
	4149	4150	4149	MS/m	
4178	4182	4180	4180	W/ms	
4191	4189	4192	4191	W/s	
4203	4200	4202	4202	M/m	S
	4212	4213	(4212)		
4223	4224		4223	M/m	
	4229	4229	4229	M/m	
(4245)	4246	4246	4246	M/mw	S
(4254)	4253	4254	4254	M/m	
(4265)	4265		(4265)		
(4278)	4280		(4280)		
4298	4299	4299	4299	M/m	
4325	4325	4327	4325	W/mw	
4340	4339	(4338)	4339	MS/s	
4343	4343	4343	4343	M/s	
4354	4352	4355	4354	MS/m	
4368	4367	4369	4368	M/mw	
(4370)		4379	(4379)		
4384			(4384)		
(4387)	4387	(4387)	(4387)		
	4391	(4392)	(4391)		
4402	4404		4403	M/m	S
4410	4409	4407	4409	M/m	S
(4420)	4420	(4417)	(4420)		
4436	4435	4438	4436	MS/w	
4454	4454	4455	4454	M/m	S
4459	4460	4460	4460	M/m	S
4471-8	4475	4475	4475	W/m	
4491		4489	(4491)		
4503	(4506)	4504	(4504)		
	(4532)	4529	(4530)		
			(4548)		
			(4576)		
(4585)	4584	4586	4585	M/w	S
(4598)	4598		(4598)		
(4610)	4612		4612	MW/ms	
	4621	4622	4621	M/m	
(4633)	4631	4632	4632	MS/m	
(4644)	4642	4643	4643	MW/ms	
(4655)	4655	4654	4654	MS/w	S
(4664)	4667	4667	4667	M/m	
	4690	4691	4690	M/w	S
	4723	4723	4723	M/mw	S
	(4734)	4736	4736	M/m	
	4754	4755	4755	MS/w	S
	4788	4790	(4789)		S
	4804	4804	4804	S/mw	
	4825-8	4828	4828	MS/w	S
	4842	4843	4843	M/w	
	4865	4865	4865	S/w	S
	4887	(4886)	(4887)		
	4898	4896	4897	M/m	
	4949	4951	4950	S/mw	S
	4962	4958	4960	M/w	S
	4975	4978	4977	S/w	S
	4991-7	4994	4995	M/w	S
	5010	5012	5011	vS/w	S
	5033	5032	5032	S/mw	S
	(5066)	5065	(5065)		
	5086	5082-5-8	5086	M/mw	S
	5094	5097	5095	M/m	S
	5104	5107	5105	MW/w	S
	(5123)	(5125)	(5124)		
	5140	(5140)	(5140)		
	(5150)	5150	(5150)		
	5160	5161	5160	S/mw	
	5198	+	(5198)		
	5226	(5227)	(5227)		S
	5280	5279	5280	vS/vw	S
	5303	5303	5303	S/w	S
	5336	5340	5338	S/w	
	5373-82	5378	5378	MW/m	
	5424	5423	5423	M/m	
	5452	5449	5481	M/m	
		*	5479	M/mw	
		*	5505	mS/mw	
		*	5836	S/mw	
		*	(5958)		
		*	6070	S/mw	

*Measured on SI 835, 856

+The region near 5200A appears to contain much structure on SI 869.

extent loses some of its attractiveness. We therefore feel that Lβ, if present at all, must be rather weak and that the feature at ~4540 Å should be attributed in the main to O VI. Two loopholes in this argument should, however, be noted. If the measured wavelength of Lα were too low, perhaps due to asymmetries caused by absorption as arises in many QSO spectra, the width and central wavelength of the O VI λ4540 feature could perhaps be understood in terms of an additional contribution from Lβ. The Digicon data, however, suggest that Lα is fairly symmetrical, and certainly neither the Digicon nor the photographic data show evidence of a strong absorption in the longward wing of the Lα emission.

TABLE 2

EMISSION-LINE CHARACTERISTICS

	Lα	Lβ + O VI
λ_c	5345	4543
W	180	52
$w_{1/2}$	58	92
w_c	118	128

The second possibility is that the O VI lines are optically thick and do not therefore have their standard 2:1 intensity ratio. This in turn would shift the rest wavelength of the line longward of 1033.8 Å, and a contribution from Lβ could then be invoked to account for the observed wavelength of the line. The maximum change in the O VI rest wavelength would be to 1034.75 Å and would then imply a maximum Lβ equivalent width of ~6 Å. From the observed equivalent width of Lα this would still imply a substantial Lβ optical depth. We note, however, that the O VI contribution would still be significantly wider than Lα, thus leaving us with the same problem as before. It appears to us that this can probably be explained in terms of mass motions in the emission-line region, the contribution to O VI sampling a wider range of velocities than Lα. Possible interpretations in terms of mass outflow are currently being investigated. A search for Lγ was inconclusive. No obvious feature could be found at the expected Lγ wavelength either

in the Digicon or image-tube data; on the other hand, with so many absorption lines a weak emission feature could readily be lost at the Digicon resolution or image-tube accuracy.

In summary, we conclude that (i) there is significant and possibly large optical depth in Lα and Lβ (ii) the feature at ~4540 Å is due mainly to O VI, and (iii) the O VI line is substantially broader than Lα and constitutes possible evidence for mass outflow in OH 471. Given that there is significant optical depth in the Lα and Lβ lines, it is in principle possible that Lyman continuum opacity may contribute to the continuum falloff around 4000 Å. This falloff is illustrated in figure 2 and clearly begins longward of the predicted Lyman continuum wavelength. The flux continues to decrease in stages to about 3875 Å, recovers briefly, and was probably not detected shortward of 3750 Å (see fig. 2). *If* it is assumed that the actual level of emission is constant shortward of 3750 Å, our data enable us to place an upper limit (3 σ) on this emission of one-fifth the value at 4000 Å. The envelope curves do, however, provide some hint of a marginal detection near 3660 Å, but this could easily be imperfect sky subtraction or simply statistical noise.

The data imply that only a relatively minor proportion of the continuum absorption shortward of 4000 Å can be due to absorption in the emission-line region. This conclusion rests on the continued decline of the observed flux shortward of the predicted Lyman continuum edge, from which we infer an upper bound to the optical depth τ_{ce} in the emission zone of $\tau_{ce} \lesssim 0.3$ even at the absorption edge. This conclusion is supported by the deficit of photons in the Lα line compared with the number removed in the Lyman continuum, although this latter argument would be void if either (i) the emission zone is nonspherically symmetric (perhaps consisting of several optically thick clouds only one of which happens to lie in the line of sight, or possibly having a disklike geometry), or (ii) the emission zone contains dust with an optical depth τ_d exceeding $\tau_{L\alpha}^{-1}$, where $\tau_{L\alpha}$ is the optical depth in Lα. (The dust-to-gas ratio implied by this latter condition is, interestingly enough, the same as that found in the interstellar medium if the emission zone is assumed to have a temperature $\sim 10^4$ ° K). We also note that the decline in the continuum emission commences longward of the Lyman limit, which may constitute evidence of strong mass motions in the emission zone.

Oke (1974*b*) has recently presented spectrophotometric data on OH 471 obtained with the multichannel scanner at the 5-m Hale telescope. Although our results give the same qualitative picture of the spectrum, quantitative agreement between the two sets of data, especially in regard to emission-line strengths, is poor. For example, Oke's equivalent widths of Lα and (Lβ + O VI) differ from ours by factors of ~3 and 0.5, respectively. In our opinion these differences may be attributed to uncertainties in locating the continuum level and to the poor resolution and inadequate sampling of the multichannel observations. For example, the (Lβ + O VI) equivalent width depends entirely on one observed point which is clearly inadequate, particularly if the feature has the broad flat-topped structure flanked by strong absorption features, found in our observations. We should also point out the discrepancy between the pronounced asymmetry in Oke's Lα profile whereas neither the Digicon nor the image-tube data show such an effect. We speculate that Oke's result may likewise be attributable to a combination of poor resolution and inclusion of N V in the emission profile. Further independent observations will, of course, be required to settle these questions.

IV. THE ABSORPTION-LINE SPECTRUM

A search has been made among the absorption lines listed in table 1 for well-defined absorption redshift systems. The results have, however, been disappointing in that we have been unable to find any "unquestionable" systems such as the system at $z = 2.309$ in PHL 957 (Lowrance *et al.* 1972) or that with $z = 1.775$ in 1331+170 (Strittmatter *et al.* 1973). As noted above, the difficulty may arise because of the great multitude of absorption features in the spectrum, many of which appear to be blends at our resolution. For example, the entire spectrum between 4950 Å and the strong feature at 5011 Å is eaten into by what appears to be a succession of overlapping absorption lines. The "blend" wavelengths would tend to give poor agreement with predicted line wavelengths in candidate redshift systems and hence result in the rejection of the line identification and possibly even of the redshift. The problem is increased in OH 471 by the smaller than average spectral range available for study owing to the falloff in intensity shortward of 4000 Å. Clearly this object requires study at higher dispersion, especially longward of 5500 Å where our present system is not of adequate sensitivity.

Probable redshift systems are listed in table 3 in increasing order of redshift, namely, $z = 3.122$, 3.191, 3.246, 3.343. None should, however, be regarded as "certain," as the number of identifications in each is not great, nor is the wavelength agreement excellent. Because of the blending problems noted above we nonetheless feel that these systems have a reasonable chance of being correct, and should in any case be subject to test when higher-resolution spectra become available.

The identification of O VI λ1031.9 in system 1 is somewhat doubtful, since the presence of the second but weaker member of the doublet at 1037.6 Å has not been clearly established. Structure has, however, been noted in the region 4278–4289 Å on two spectrograms, and it is possible that this is, in part, due to the O VI λ1031.9 feature. It is also possible that C III λ977, Si III λ1206 may contribute to the wide features at 4032 and 4977 Å, respectively. A recent spectrogram SI 1135 centered at 5800 Å with a dispersion of 240 Å mm^{-1} shows an absorption feature at 6385 Å which may be due to C IV λ1550 in this system, but this point requires confirmation.

In system 2 we note that the wavelength agreement for Lγ and Lδ is rather poor, although both features

TABLE 3

PROBABLE ABSORPTION REDSHIFT SYSTEMS

Line	λ_{rest}	λ_{obs}	character	1 + z
System 1	z = 3.122			
Lγ	972.5	4007	MS/mw	4.120
Lβ	1025.7	4229	M/m	4.123
OVI	1031.9	4254	M/m	4.123
Lα	1215.7	5011	vS/w	4.122
NV	1238.8	5105	MW/w	4.121
NV	1242.8	(5124)		(4.123)
SiII	1260.4	(5198)		(4.124)
System 2	z = 3.191			
Lδ	949.5	(3984)		4.194
Lγ	972.5	4073	MS/w	4.188
CIII	977.6	(4094)		4.190
OI	988.8	4145	MS/m	4.192
NIII	989.8	4149	MS/m	4.191
SiII	989.9			
Lβ	1025.7	4299	M/m	4.191
CII	1036.3	4343	M/s	4.191
NI	1134.6	4755	MS/w	4.191
NI	1199.9	5032	S/mw	4.194
Lα	1215.7	5085	M/m	4.191
SiII	1260.4	5280	vS/vw	4.189
System 3	z = 3.246			
Lε	937.8	(3984)		4.248
Lδ	949.7	4032	S/w	4.246
Lγ	972.5	4130	M/m	4.247
CIII	977.0	4145-4149	MS/m	4.245
NIII	989.8	4202	M/m	4.245
Lβ	1025.7	4354	MS/m	4.245
Lα	1215.7	5160	S/mw	4.245
System 4	z = 3.343			
Lε	937.8	4073	MS/m	4.343
Lδ	949.7	4121	M/m	4.345
Lγ	972.5	4223	M/m	4.342
CIII	977.0	4246	M/mw	4.346
NIII	989.8	4299	M/m	4.343
Lβ	1025.7	4454	M/m	4.342
Lα	1215.7	5280	vS/vw	4.343

are rather broad and may thus be composite. The possible identifications with O I λ988.8 and C II λ1036.3 could normally be confirmed by the presence of O I λ1302.2 and C II λ1334.4, but these are unfortunately confused with the nightsky Hg I λ5461 and O I λ5577 emission features. The suggested identification with N III λ989.9 is supported by the presence of C III, but the apparent absence of N II λ1084.0 is somewhat disturbing. The features should, however, appear at ~4543 Å, near the O VI peak, and may therefore have been missed. Alternatively the feature at 4149 Å may be due to Si II λ989.9, implying that other Si II features should also be present. The strongest line at 1260.4 Å could indeed be contributing to the broad feature at 5280 Å, and the lines at 1190.4 and 1193.3 Å may likewise be unresolved members of the broad absorption between 4950 and 5011 Å. Higher-dispersion spectrograms may settle this question. The only remaining line of Si II in our spectral range, Si II λ1304.4, would be confused with the nightsky Hg I λ5461 feature. The lines so far identified in system 2 are predominantly of lower ionization, and the possibility therefore arises that Fe II lines may be present. Grewing and Strittmatter (1973) tabulated the strongest far-ultraviolet Fe II lines, and these, together with possible identifications, are listed in table 4. While not conclusive, the evidence certainly suggests that Fe II may be present; only for very broad observed features is the wavelength agreement poor.

Systems 3 and 4 rest primarily on identifications with lines of the Lyman series. In both cases all lines up to Lε are present, indicating a high ($\gg 10^2$) optical depth in Lα. In system 3 the feature at 4202 Å might be identified with Si II λ989.9, while that at 5065 Å would correspond to Si II λ1193.3. The absence of Si II λλ1190.4 and 1260.4 (possibly partially responsible for the broad feature at λ5340) renders interpre-

TABLE 4

EVIDENCE FOR Fe II ABSORPTION IN SYSTEM 2

Fe II λ_{rest}	λ_{obs}	Character	1 + z
1064.0.....	4460	M/m	4.192
1096.9.....	(4598)	...	4.192
1133.7.....	4754	MS/w	4.193
1142.3.....	(4789)	...	4.192
1145.0.....	4804	S/mw	4.196
1260.5.....	5280	vW/vw	4.189

tation in terms of Si II rather difficult. For system 4 the same problem arises for the line at 4299 Å, but N III λ989.8 is clearly preferred in this case because no other Si II features are observed.

The predicted Lyman continuum wavelengths for systems 1–4 are also noted in figure 2. Although the data are not adequate to draw any firm conclusions at present, they do suggest that the continuum declines in stages at wavelengths corresponding approximately to the Lyman continuum edge in the case of at least three of the four suggested redshift systems. This would imply column densities of neutral hydrogen $N_H \sim 10^{17}$ cm^{-2} in each of the absorbing clouds. The observed absorption line strengths indeed provide further support for this suggestion. The detection of strong Lα in systems 3 and 4 implies a column density of neutral hydrogen $N_H \gtrsim 10^{17}$ cm^{-2} in each of these clouds; some absorption from the Lyman continuum is almost inevitable. It seems to us, therefore, that most of the absorption shortward of 4000 Å should be ascribed to the clouds giving rise to the observed absorption line systems. If so, the intermediate optical depth in the Lyman continuum may provide important clues as to the origin of these absorbing clouds.

We note that the number of photons in Lα emission is apparently substantially less than the number absorbed in the continuum. Because of the substantial velocity difference between the absorption and emission regions, however, these photons would be received over the wavelength range 5000–5700 Å if the absorption regions were spherically symmetric. The photons would be considerably more difficult to detect, so this deficit cannot be established with any great degree of certainty. Neither the present data nor those of Oke (1974*b*), however, show any evidence for these extended Lα contributions. If correct, this would argue against a spherically symmetric distribution of absorbing matter (either in shells or in many discrete clouds[1]) near the QSO, unless (cf. § III) dust is present in sufficient quantity to suppress the Lα photons. An alternative explanation is that the absorbing clouds are nonspherically distributed around the QSO, perhaps in a disk. Finally, one may postulate that the absorption occurs in clouds at great distance ($> 10^2$ kpc) from the QSO so that much of the Lα emission contribution from scattered photons is not detected. A particular version of this hypothesis, namely, that the absorption arises in intervening galaxies, is clearly consistent with the present data. If this hypothesis is generally correct for QSO absorption systems, then, by analogy with other QSOs, a number of absorption systems with redshifts in the range $2.0 \leqslant z \leqslant 3.0$ would be expected in OH 471. A search for such systems was therefore undertaken and will be described below.

In addition to the above "probable" absorption redshift systems, we wish to note certain other "possible" systems for which the evidence is weaker. These cases are listed in table 5 and have been retained mainly because of their interest in relation to specific questions. For example, a search was made among the "definite" lines in table 1, for line ratios corresponding to the Lα/Lβ ratio. Four further cases (in addition to those in table 3) were found and would correspond to redshifts of 2.971, 3.028, 3.139, and 3.362, respectively. While these may be real, no convincing supporting evidence could be found for any but the first, which is accordingly listed in table 5. A close examination of SI 850 and 869 provided some evidence for the presence of N V at the same redshift.

An attempt was also made to identify as Lα the absorption line at 5340 Å (in Lα emission) implying a redshift $z = 3.3925$; no supporting evidence could, however, be found. On the other hand, there is some support for an identification with C IV λ1550 at a redshift of 2.447 (see table 5). The weakness of Lα and the absence of Si IV λ1402.8 (there is some suggestion of a feature on SI 869) render this identification rather unlikely.

In analyzing the data in table 1, the group of lines consisting of λλ4621, 4632, 4643, 4655, and 4667 stands out because, to within measuring errors, successive ratios are equal. This ratio (1.0024–1.0026) corresponds closely to that of the Si II λλ1190.4, 1193.3 pair (1.00244) and the Mg II λ2798 doublet (1.00258). Identification with Mg II yields four redshifts $z = 0.653, 0.657, 0.661$, and 0.665. In an attempt to seek confirmation of any of these, a search for Fe II lines was carried out. Possible identifications with Fe II λ2599.4 at $z = 0.653$ and with Fe II λ2585.9 at $z = 0.665$ were found. In no case were both features present. The stronger Fe II features at shorter wavelengths would unfortunately be below 4000 Å, so they cannot be used as further tests. Although Mg II has been seen only rarely in absorption in QSO spectra, it is interesting that a twin overlapping system containing this doublet has been observed in 1331+170 (Strittmatter *et al.* 1973). The above redshift systems are, however, very uncertain and should be viewed merely as suggestions.

Identification with the Si II doublet yields redshifts of 2.882, 2.891, 2.901, 2.911. Little supporting evidence (e.g., Lα, Si II λ1260.4) could be found for the first three redshift systems. Several identifications are, however, possible at redshifts of around 2.911, and these are listed in table 5. The absence of a clear-cut feature corresponding to Si II λ1260.5 is the main argument against this system, especially as the redshift was based originally on the identification of the Si II λλ1190.4, 1193.3 pair. The scatter in z is also rather larger than is normally acceptable, but the results almost suggest a bimodal distribution with redshifts 2.906 and 2.916. A reexamination of the plates suggests that some of the "single" features listed in table 1 may indeed be double. Higher-resolution spectrograms will, however, be required to settle this question. It is perhaps worth noting that within the redshift range 2.882–2.910 there seem to be a number of "near miss" redshift systems, an example of which, $z = 2.855$, is also listed in table 5. Although we

[1] In view of the number of absorption clouds in the line of sight, it seems unreasonable to assume that there is much incompleteness of absorption of continuum radiation by the clouds, if they have roughly a spherical distribution.

TABLE 5

POSSIBLE ABSORPTION REDSHIFT SYSTEMS

Line	λ_{rest}	λ_{obs}	character	1 + z	Comments
z = 0.805					
FeII	2343.5	4229	M/m	1.805	
FeII	2382.0	4299	M/m	1.805	
FeII	2585.9	4667	M/m	1.805	
FeII	2599.4	4690	M/w	1.804	
MgII	2795.5	--			Possible feature at 5046A on SI 857
MgII	2802.7	5065		1.807	
z = 2.015					
SiIV	1393.8	4202	M/m	3.015	
SiIV	1402.8	4229	M/m	3.015	
CIV	1548.2	4667	M/m	3.014	
CIV	1550.8	--			Possible feature at 4675A on SI 869
z = 2.447					
Lα	1215.7	4191	W/s	3.447	
SiII	1260.4	4343	M/s	3.446	
SiIV	1393.8	4804	S/mw	3.447	
CIV	1549	5340	S/w	3.447	
z = 2.491					
Lα	1215.7	4246	M/mw	3.493	
NV	1238.8	4325	W/mw	3.491	
NV	1242.8	4339	MS/s	3.491	
SiII	1260.4	4403	M/m	3.493	
SiIV	1393.8	4865	S/w	3.490	
SiIV	1402.8	4897	M/m	3.491	
z = 2.911					
Lβ	1025.7	4007	MS/mw	3.907	4011 A on SI 957 z = 3.911
OVI	1031.9	4032	S/w	3.907	Possibly double
OVI	1037.6	(4056)	--	3.909	
AII	1048.2	(4100)	--	3.911	
NII	1084.0	4246	M/mw	3.916	
SiII	1190.4	4655	MS/w	3.910	
SiII	1193.3	4667	M/m	3.911	
NI	1199.9	4690	M/w	3.909	
SiIII	1206.5	4723	M/mw	3.915	
Lα	1215.7	4755	MS/w	3.911	Possible components at 4749A (z=2.906) and at 4763A (z=2.917)
NV	1238.8	4843	M/w	3.909	Possible component at 4839A (z=2.906)
NV	1242.8	4865	S/w	3.914	Too strong
SiII	1260.4	--	--	--	Complex structure. Possible features at 4923A (z=2.906) and 4936A (z=2.916)
OI	1302.2	5095	M/m	3.913	Too strong, possibly SiII 1304 (z=2.906)
SiII	1304.4	5105	MW/w	3.914	Possibly also 5095 (z = 2.906)
CII	1334.5	5226	--	3.916	Possible feature at 5214 (z=2.907)
CIV	1550.8	~6070	S/mw	(3.914)	
z = 2.971					
Lβ	1025.7	4073	MS/m	3.971	
OVI	1031.9	4100	--	3.973	
OVI	1037.6	4121	M/m	3.972	
Lα	1215.7	4828	MS/w	3.971	

cannot claim to have established the point, it has seemed to us as though different lines and/or ions have slightly different velocities, indicating perhaps differential flow in the absorbing cloud.

We have made a special search for absorption systems with relatively low ($z < 3$) redshifts, since on the intervening-galaxy hypothesis for the origin of absorption lines in QSOs (Bahcall 1971) many such systems would be expected. No clear-cut cases have been found. We should, however, reiterate the increased difficulty of finding such systems within the shorter observable spectral range and with the frequent line blending found in OH 471. Apart from the tentative cases already discussed, candidate systems were found at redshifts $z = 0.805$, 2.015, 2.491; these are again listed in table 5. The Fe II identifications at $z = 0.805$ are satisfactory, but the absence of Mg II λ2795 is disconcerting. A reexamination of the plates showed a possible feature at 5046 Å on SI 857, but further observations are required to ascertain its reality. The implied ratio of the Mg II line strengths also argues against this system. The absence of C IV

λ1550.8 similarly casts doubt on the $z = 2.015$ system, although again a weak feature was measured at 4675 Å on plate SI 869. The system at $z = 2.491$ is also doubtful in view of the relative strengths of the N V lines and the absence of other Si II lines (λ1260.4 is, however, the strongest expected line). Detection of the C IV λ1549 doublet would greatly enhance the possibility that this system is real, but our present data are inadequate to the task. The presence of low-redshift systems thus remains in doubt. Further observations at higher resolutions are planned for next season with a view to settling these questions.

Finally a limited search was carried out for absorption lines arising from fine-structure levels of the ground state in each of four probable redshift systems. No clear-cut case could, however, be established.

V. SUMMARY

Digicon and image-tube spectroscopy of OH 471 indicate:

i) The Lα emission is probably optically thick and the emission line at 4540 Å is due in the main to O VI.

ii) The width of the O VI line is greater than Lα, suggesting different gas motions in the regions producing the two lines.

iii) Four probable absorption-line redshift systems ($z_{abs} = 3.122$, 3.191, 3.246, 3.343) have been found among the 89 absorption lines established in OH 471. Several more possible systems have been suggested.

iv) The continuum absorption shortward of 4000 Å is probably due to Lyman continuum absorption in gas giving rise to the absorption-line redshift systems.

v) The absorption spectrum is so rich that substantially higher spectral resolution is required to identify the absorption lines. This is especially important in the quest for lower-redshift ($1.5 \leq z \leq 2.5$) absorption systems, of which none have so far been established with certainty but which must be present if the cosmological redshift interpretation is correct.

vi) There is some evidence for nonspherical geometry and/or dust absorption in OH 471.

We are aware that our results are so far disappointingly ambiguous but feel nonetheless that the evidence should be presented as it stands.

We are indebted to E. M. Burbidge, A. Boksenberg, F. Hoyle, C. E. McIlwain, J. B. Oke, E. J. Wampler, and R. J. Weymann for helpful discussions on various aspects of this work, which has been supported at Steward by the NSF (grant GP-32450) and NATO (grant N0647) and at San Diego by NASA. One of us (P. A. S.) wishes to thank Professor L. Biermann for hospitality at the Max Planck Institute for Physics and Astrophysics, Munich, where part of this investigation was carried out. We also wish to acknowledge assistance from the Steward Observatory Mountain staff and the invaluable contributions of R. Cromwell and R. Hilliard in maintaining and improving the equipment.

REFERENCES

Bahcall, J. 1971, *A.J.*, **76**, 283.
Beaver, E. A., and McIlwain, C. E. 1971, *Rev. Sci. Instr.*, **42**, 1321.
Browne, I. W. A., Crowther, J. H., and Adgie, R. L. 1973, *Nature*, **244**, 146.
Carswell, R. F., and Strittmatter, P. A. 1974, *Nature*, **242**, 394.
Gearheart, M. R., Lund, J. M., Frantz, D. J., and Kraus, J. D. 1972, *A.J.*, **77**, 557.
Grewing, M., and Strittmatter, P. A. 1973, *Astr. and Ap.*, **28**, 39.
Lowrance, J. O., Morton, D. C., Zucchino, P., Oke, J. B., and Schmidt, M. 1972, *Ap. J.*, **177**, 219.
Oke, J. B. 1974*a*, *Ap. J.* (*Suppl.*), **27**, 21.
———. 1974*b*, *Ap. J.* (*Letters*), **189**, L47.
Strittmatter, P. A., Carswell, R. F., Burbidge, E. M., Hazard, C., Baldwin, J. A., Robinson, L., and Wampler, E. J. 1973, *Ap. J.*, **183**, 767.

E. A. BEAVER and R. HARMS: Department of Physics, University of California–San Diego, La Jolla, CA 92037

R. F. CARSWELL: Department of Physics and Astronomy, University College, London, Gower Street, London, England

P. A. STRITTMATTER and R. E. WILLIAMS: Steward Observatory, University of Arizona, Tucson, AZ 85721